

TOWARDS THE VALIDATION OF SeaWiFS IN SOUTHERN AFRICAN WATERS: THE EFFECTS OF GELBSTOFF

S. BERNARD*, T. A. PROBYN† and F. A. SHILLINGTON*

The effective application of future ocean colour data for southern African waters requires an in-depth assessment of bio-optical algorithm performance, given the productive and highly variable nature of the oceanographic region. Phytoplankton degradation products, commonly known as gelbstoff, represent a large potential error source to future remotely sensed chlorophyll data, particularly in highly productive regions, where there can be a dramatic lack of covariance between phytoplankton and gelbstoff concentrations. Data relevant to gelbstoff character in the Agulhas Bank and southern Benguela systems are examined to assess the variability of gelbstoff chromophoric structure in these regions. These take the form of gelbstoff absorption spectra, and fluorescence excitation-emission matrices, performed on filtered seawater samples. Modelled bio-optical data, using conditions typical of high biomass marine environments, are then used to assess the performance of a proposed SeaWiFS combined algorithm with respect to variations in the magnitude and nature of gelbstoff absorption. It is shown that expected algorithm performance can be poor in bloom type scenarios, and that an appreciation of algorithm application is needed for effective interpretation of ocean colour imagery.

The recent availability of data from a new generation of ocean colour sensors, such as the Seaviewing Wide Field-of-view Sensor (SeaWiFS) has stimulated the need for a greater understanding of the bio-optical processes fundamental to the interpretation of remotely sensed ocean colour. One of the most pressing problems in marine science is the need for a greater knowledge of large scale biogeochemical cycles. Remotely sensed ocean colour has the potential to provide unique information on the scales of these cycles in the upper ocean, offering rapidly and frequently acquired synoptic biogeochemical data. However, the truly productive use of ocean colour data across a diversity of marine systems will only be achieved if the optically significant components in the marine environment can be effectively characterized, and the biogeochemical processes integral to them understood. This is particularly necessary in view of the development of new generation phytoplankton biomass algorithms, which have progressed from the empirical Coastal Zone Colour Scanner (CZCS) pigment variety (Gordon and Morel 1983) to potentially more accurate semi-analytical chlorophyll *a* variants, such as those to be used with the more sensitive SeaWiFS sensor (Carder *et al.* 1991, 1995). If these algorithms, dependent as they are on the application of idealized bio-optical parameters, are to be used in highly productive areas such as shelf seas, then it is imperative that they are not used indiscriminately. Core bio-optical parameters, their effects on the underwater light-field, and the ways these impact ocean colour products must

be evaluated for areas of interest. Assessment of the accuracy of global pigment algorithms is a primary goal, with particular regard to the effects of site- and season-specific variations from the idealized bio-optical parameters such algorithms necessarily use. A secondary, though no less important, objective is improving the understanding of core bio-optical and related biogeochemical processes, allowing ocean colour imagery to yield maximum information through a process-driven approach.

The principle determinants of ocean colour in the world's oceans can be considered to be phytoplankton and their associated degradation products (Gordon and Morel 1983, Carder *et al.* 1989, 1991, 1995). In areas with strong terrestrial and anthropogenic influences, suspended sediment and allochthonous dissolved material must be accounted for, but such cases must be considered on a site-specific basis (Gordon and Morel 1983, Carder *et al.* 1989). Strong emphasis is placed on a thorough understanding of complex autochthonous processes from a bio-optical perspective. These processes can be regarded as having three main bio-optical components: the phytoplankton, tripton (non-living particulate matter of biological origin), and dissolved organic degradation products, variously known as gelbstoff, chromophoric dissolved organic matter (CDOM), yellow substance, gilvin, and marine humic substances. The importance of gelbstoff stems from its significant and widespread contribution to light absorption in the sea (Siegel and Michaels 1996)

* Department of Oceanography, University of Cape Town, Rondebosch 7701, South Africa. Email: bernard@physcu.udt.ac.za

† Sea Fisheries, Private Bag X2, Rogge Bay 8012, South Africa. Email: tprobyn@sfri.wcape.gov.za

Table I: Glossary of variables used

Symbol	Definition
λ	Wavelength of light (nm)
λ_r	Gelbstoff reference wavelength (nm)
A	Absorbance or optical density
a_g	Gelbstoff absorption coefficient (m^{-1})
a_g^s	Gelbstoff absorption shape parameter (m^{-1})
a_ϕ	Phytoplankton absorption coefficient (m^{-1})
a_ϕ^s	Chl <i>a</i> specific phytoplankton absorption coefficient ($\text{m}^{-2}\text{mg chl } a^{-1}$)
a_w	Seawater absorption coefficient (m^{-1})
b_p^p	Particulate backscattering coefficient (m^{-1})
b_w^p	Seawater backscattering coefficient (m^{-1})
$C_{chl a}$	Chlorophyll <i>a</i> concentration ($\text{mg}\cdot\text{m}^{-3}$)
b_p^p	Particulate backscattering coefficient (m^{-1})
b_w^p	Seawater backscattering coefficient (m^{-1})
L_{WN}	Normalized water leaving radiance ($\text{W}\cdot\text{m}^{-2}\text{nm}^{-1}\text{sr}^{-1}$)
$rC_g(n)$	Relative gelbstoff concentration vector
R_{rs}	Remotely sensed reflectance
S	Gelbstoff slope parameter (nm^{-1})
d	Path length (m)

and its role in the cycling of dissolved organic carbon DOC (Druffel *et al.* 1992) through its majority components, dissolved humic and fulvic acids (Ehrhardt 1984, Carder *et al.* 1989, 1991). The collective of organic substances that constitute gelbstoff absorbs light in a characteristic manner, decreasing exponentially with wavelength from a maximum in the ultraviolet. This lends itself to the following mathematical description of gelbstoff absorption (e.g. Bricaud *et al.* 1981, Carder *et al.* 1991). (See Table I for a glossary of the variables used.)

$$a_g(\lambda) = a_g(\lambda_r) e^{S(\lambda_r - \lambda)} \quad (1)$$

This characterization allows gelbstoff absorption to be described by two parameters: absorption at a reference wavelength $a_g(\lambda_r)$, and the slope parameter S . The effects of gelbstoff on the underwater light-field, and ultimately satellite-derived chlorophyll measurements, will be manifest in the variation of these two parameters, particularly $a_g(\lambda_r)$. The relationship between phytoplankton biomass and $a_g(\lambda_r)$, as a proxy for gelbstoff concentration, is particularly important. Covariance between phytoplankton and its degradation products is a central criterion for qualification as a Case I water type (Morel 1988). However, there can be a significant lack of covariance between phytoplankton biomass and gelbstoff, even in archetypal Case I waters such as the Sargasso Sea (Siegel and Michaels 1996). This phenomenon is likely to be most dramatic in highly productive, pulsed upwelling systems such as the Benguela, where the rapid growth and decay of phytoplankton blooms can lead to rapid changes in the phytoplankton:

gelbstoff ratio (Peacock *et al.* 1988, Carder *et al.* 1989). Periods around bloom senescence are perhaps particularly sensitive to large and rapid changes in chlorophyll concentrations and both $a_g(\lambda_r)$ and S , as phytoplankton populations collapse, producing substantial quantities of organic compounds in intermediate stages of humification. The composition of gelbstoff in these periods is liable to be atypical, consisting of labile compounds, with relatively high ratios of humic acids to fulvic acids (Harvey *et al.* 1983, Carder *et al.* 1989). Fulvic acids typically constitute 90% or more of total humic substances and therefore dominate net gelbstoff absorption. However, small increases in the humic acid fraction will result in net gelbstoff absorption displaying typical humic acid characteristics, i.e. flatter slope parameters (lower S) and increased mass or carbon specific absorption (Hayase and Tsubota 1985, Carder *et al.* 1989, 1991). Such phenomena may not only exaggerate short-term variations in the phytoplankton: gelbstoff ratio through increases in $a_g(\lambda_r)$, but result in divergence from the fixed S utilized by semi-analytical chlorophyll algorithms.

Other fundamental bio-optical variables, such as chlorophyll-specific phytoplankton absorption (Bricaud *et al.* 1995) and backscattering (Morel 1988), will also need validation in southern African waters or, at the very least, an appreciation of their possible effects through regional divergence (Carder *et al.* 1995). However, understanding the effects of gelbstoff, as a ubiquitous and potentially highly variable component of the marine light-field, must be an important objective in the southern African regional validation of sensors such as SeaWiFS.

RATIONALE

An examination of the nature and potential effects of gelbstoff in southern African waters will be made, using two separate approaches. First, available data relevant to gelbstoff character in the southern African region will be examined to assess the nature of gelbstoff in areas such as the Agulhas Bank and the southern Benguela. These data, derived from surface waters from the South African south and west coasts, take the form of gelbstoff absorption and fluorescence excitation-emission matrices (EEMs), a descriptive means of analysing the source and chromophoric structure of DOM (Coble *et al.* 1990, 1993, Mopper and Schultz 1993, Coble 1996). The second section of the study will assess the performance of a proposed SeaWiFS combined algorithm (Carder *et al.* 1991, 1995) using appropriately constrained, modelled bio-optical data to

generate reflectance data as algorithm input. Focusing on the effects of gelbstoff, the model examines the effects of variations in both $a_g(\lambda)$ and S through a range of concentrations of chlorophyll a , allowing the relative performance of the algorithm to be monitored through a wide range of bio-optical scenarios. This approach permits an appreciation of algorithm response to changes in gelbstoff parameters at different biomass levels, despite the paucity of bio-optical data from southern African waters. It should be emphasised that *bona fide* validation of SeaWiFS algorithms must be based on appropriate *in situ* bio-optical measurements.

METHODS

Surface water samples for absorption and fluorescence data were taken in the vicinity of the Agulhas Ridge on 3 and 5 March 1994, and approximately 60 km north-west of St Helena Bay on May 1994. Samples were filtered through pre-rinsed, ashed GF/F filters and frozen at -20°C until analysis. Absorption measurements were made with a Hitachi U-2000 UV/VIS double-beam scanning spectrophotometer, with 40 mm quartz cuvettes and Milli-Q water as reference. Absorbance was measured from 250 to 650 nm at 5-nm intervals, and a refractive index correction applied by subtracting absorbance at 650 nm from all data (Green and Blough 1994). Corrected data were then converted to absorption coefficients through Equation 2 (Mueller and Austin 1995):

$$a(\lambda) = 2.303 \frac{A(\lambda)}{d} \quad (2)$$

Absorption data from 250 to 650 nm were then fitted to Equation 1 using a non-linear least squares regression technique (Statgraphics V6.0) to determine S , using $\lambda_r = 400$ nm. These regressions yielded r^2 values >0.99 in all cases.

Fluorescence measurements were made by means of a Hitachi F-4000 fluorescence spectrophotometer operating in corrected mode, using excitation and emission bandpasses of 10 nm, a scan speed of $120 \text{ nm}\cdot\text{min}^{-1}$ and a 10-mm quartz cuvette. A blank fluorescence scan of Milli-Q water was subtracted from all data to remove Rayleigh and Tyndall scattering peaks. Excitation-emission matrices were produced using Surfer for Windows V6 (Golden Software), with excitation wavelengths of 250–400 nm and emission wavelengths of 260–500 nm. Generated surface plots were overlaid

with filled contours representing plan curvature, with Z-axis units of relative fluorescence (Fig. 1).

MODEL STRUCTURE

The bio-optical model uses Equation 3 (Carder *et al.* 1991) to produce the remotely sensed reflectance (R_{rs}) values needed for input to the algorithm:

$$R_{rs} = 0.33(b'_w + b'_p)/(a_w + a_g + a^*_\phi [C_{chl\ a}]) \quad (3)$$

The spectral dependence of terms is omitted for convenience. Two assumptions given below are implicit to Equation 3, in itself an approximation.

- (i) The constant term (0.33) is based upon simplifications concerning the angular distribution of the underwater light field (Morel 1988) and assumes approximate zenith sun.
- (ii) Transpectral effects arising from *in situ* DOM fluorescence and water Raman scattering are negligible (Carder *et al.* 1991. Lee *et al.* 1994).

The derivation, structure and rationale for the various parameters used in the model are described below.

Phytoplankton absorption coefficients (a_ϕ and a^*_ϕ)

Data for these variables are produced using the appropriate expression from the tested algorithm, thus minimizing possible divergence arising from variations in a^*_ϕ , because the focus of this study is gelbstoff-related divergence effects. It should be noted that *in situ* values of this parameter are prone to a high degree of variation with taxonomy, and light and nutrient history (Carder 1994, Bricaud *et al.* 1995). However, this issue must be dealt with specifically, and the functions used here are contrived to prevent effects arising from variations in phytoplankton absorption. The semi-analytical inversion procedure used in the algorithm employs $a_\phi(675)$ as a necessary intermediate variable between chlorophyll a concentration and phytoplankton absorption, and $a_\phi(\lambda)$ is an expression of $a_\phi(675)$ (Carder *et al.* 1995):

$$a_\phi(\lambda) = a_\phi(675) e^{[a_1(\lambda) \tanh[a_2(\lambda) \ln(a_\phi(675)/a_3(\lambda))]]} a_\phi(675) \quad (4)$$

The relationship between $C_{chl\ a}$ and $a_\phi(675)$ is expressed as:

$$C_{chl\ a} = p_0 a_\phi(675) P_1 \quad (5)$$

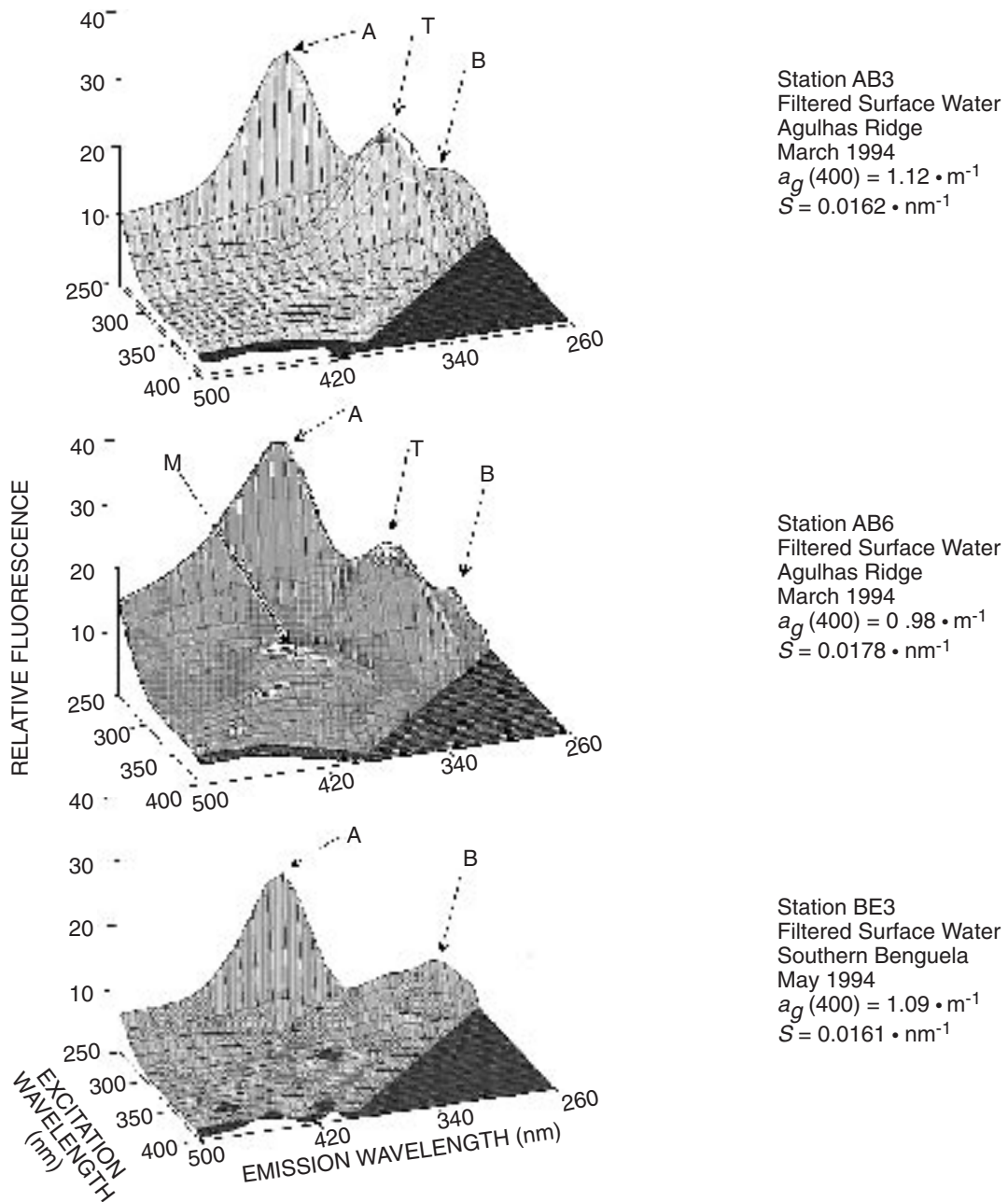


Fig. 1: Fluorescence excitation-emission matrices and gelbstoff absorption data from the Agulhas Bank and the southern Benguela. Note the predominance of ultra-violet fluorescence, indicative of recent autochthonous formation

Table III: Location and description of major fluorescent components (after Coble 1996)

Peak	Sample ($\lambda_{\max_{\text{excitation}}}$ / $\lambda_{\max_{\text{emission}}}$)				Fluorophore
	AB3	AB6	BE3		
B Intensity	250/290 9.8	250/290 9.7	250/290 7.4		Tyrosine-like
T Intensity	270/330 19.5	260/330 19.3	–		Tryptophan-like
A Intensity	250/390 30.3	250/400 36.1	250/390 24.3		Humic-like
M Intensity	–	310/410 9.1	–		Marine humic-like

The proposed SeaWiFS combined algorithm

Algorithm code was obtained from S. Hawes of the University of South Florida in July 1996. The algorithm essentially consists of two sections: a semi-analytical algorithm designed to calculate chlorophyll *a* concentrations through the intermediate variables of $a_g(675)$ and $a_g(400)$ (Carder *et al.* 1991, 1995, Carder 1994), and a default CZCS-style algorithm used when the primary algorithm cannot find a suitable match of $a_g(675)$ and $a_g(400)$. This empirically derived algorithm takes the form:

$$C_{chl\ a} = 10^{C_0 + C_1 \log\left(\frac{R_{rs}(490)}{R_{rs}(555)}\right) + C_2 \left(\log\left(\frac{R_{rs}(490)}{R_{rs}(555)}\right)\right)^2} \quad (10)$$

The constants C_0 , C_1 and C_2 were assigned the values 0.289, -3.2 and 1.2 respectively (Carder *et al.* 1995).

The regional derivations of Equation 10 and the increased probability of semi-analytical algorithm failure in highly absorbing waters (Carder *et al.* 1995), such as those under consideration here, emphasizes the need for distinction between the outputs from the two algorithms.

Model usage

Two sets of data were generated for algorithm input. The first was intended to assess the effects of changing both $a_g(\lambda)$ and S over a wide range of $C_{chl\ a}$ values. Three $C_{chl\ a}$ values of 0.5, 5.0 and 25.0 $\text{mg}\cdot\text{m}^{-3}$ were each assigned three ranges of $a_g(\lambda)$ values, as determined by Equations 6, 7 and 8, with S values of 0.012, 0.017 and $0.020\cdot\text{nm}^{-1}$. An S value of $0.017\cdot\text{nm}^{-1}$ is the default value for the semi-analytical algorithm, whereas an S value of $0.012\cdot\text{nm}^{-1}$ represents a possible humic-acid-dominated scenario (Carder *et al.* 1989) and

$0.020\cdot\text{nm}^{-1}$ a feasible high slope value (e.g. Green and Blough 1994). The second dataset was designed to provide a closer examination of algorithm response in the $C_{chl\ a}$ range of $0.5\text{--}5\ \text{mg}\cdot\text{m}^{-3}$, as initial model runs show that it is within this range that the semi-analytical algorithm fails and output defaults to empirically derived $C_{chl\ a}$ through the use of Equation 10. This dataset employs a $C_{chl\ a}$ range of $0.5\text{--}4.5\ \text{mg}\cdot\text{m}^{-3}$, in increments of $0.5\ \text{mg}\cdot\text{m}^{-3}$, with $a_g(\lambda)$ ranges derived as with the first set, and a constant value of $S = 0.017\cdot\text{nm}^{-1}$.

RESULTS AND DISCUSSION

Fluorescence and absorption data

The EEMs and corresponding gelbstoff absorption parameters are shown in Figure 1. The location of peaks corresponding with the activity of major fluorophore groups compare well with published data (Coble *et al.* 1990, 1993, Mopper and Schultz 1993, Coble 1996) and are annotated after Coble (1996), as shown in Table III. A prominent characteristic of all samples is the high degree of fluorescent activity at shorter wavelengths, i.e. in the ultra-violet (UV), relative to the longer visible wavelengths. This is considered characteristic of recently produced autochthonous marine material, by virtue of the “blue-shift” in fluorescence resulting from the typically less aromatic structures of marine humic material (Coble 1996). The strong presence of Feature T, associated with the monoaromatic amino acid tryptophan, and the weak presence of Feature B, similarly associated with tyrosine, can also be considered typical of marine surface waters (Mopper and Schultz 1993, Coble 1996), particularly those containing material of recent planktonic origin (De Souza Sierra *et al.* 1994). Feature A is prominent in all samples, and can be identified as “humic-like”; it is notable that longer wavelength

“humic-like” features, e.g. Peak C (Coble 1996), do not appear in any samples, providing further evidence of a purely oceanic environment, at least as concerns the production of DOM (De Souza Sierra *et al.* 1994, Coble 1996). Feature M, which appears only in Sample AB6, is also considered typical of recent marine autochthonous material (Coble 1996) and may be the β''_A absorption band of De Souza Sierra *et al.* (1994), thought to be representative of an oceanic fluorophore. The absence of Feature T in the West Coast sample BE3 is worth noting. Although the reason for this is unknown, it further underlines the variability of fluorophore structure in this area found by Determann *et al.* (1994).

While the relationship between fluorophore structure and absorption is complex and not clearly understood, strong empirical correlations between absorption and fluorescence have been shown (Ferrari and Tassan 1991, Hoge *et al.* 1993, Green and Blough 1994). Unfortunately, the limited size of the current dataset precludes any further investigation of this relationship. However, the degree of variation in the fluorescence EEMs and the inherent link between fluorescence and spectral absorption bands (Donard *et al.* 1987, De Souza Sierra *et al.* 1994) argues for an accompanying variation in surface water gelbstoff absorption. The $a_g(400)$ values for the three stations can be considered high for oceanic environments (Green and Blough 1994), and there appears to be some variation in the slope parameter, although all three values are close to the default algorithm value of $0.017 \cdot \text{nm}^{-1}$ (Carder *et al.* 1995). It might be argued that the appearance in Sample AB6 of fluorophore M (Fig. 1), previously associated with autochthonous DOM UV absorption bands (De Souza Sierra *et al.* 1994, Coble 1996), affects the relatively high slope parameter of this sample ($0.0178 \cdot \text{nm}^{-1}$), but such an hypothesis would require confirmation from a larger dataset. Nevertheless, based on previously observed fluorescence variability (Determann *et al.* 1994) and that reported here, it would appear that the chromophoric structure of DOM in southern African surface waters is subject to a high degree of variability.

Algorithm output and results

Algorithm output can be seen in Figures 2 and 3. Algorithm performance deteriorates notably at high concentrations of chlorophyll *a*, with all returned values based on the default CZCS-style algorithm at $C_{chl\ a} = 25 \text{ mg} \cdot \text{m}^{-3}$ (Fig. 3c). It appears that chlorophyll *a* concentrations of approximately $3 \text{ mg} \cdot \text{m}^{-3}$ represent the upper working limits of the semi-analytical algorithm, with a dramatic decrease in the number of returned values above this concentration (Fig. 2). The

lack of sensitivity to variation in absorption at high absorption values is an inherent function of the reflectance Equation 3, arising from the reciprocal relationship between reflectance and total absorption (Carder 1994). The structure of the two algorithm types also results in a different response to increased gelbstoff absorption, as can be seen in Figure 2. The semi-analytical algorithm appears to function most accurately at intermediate to high gelbstoff absorption levels, at least considering the range of gelbstoff data employed in this bio-optical model. The CZCS-type algorithm, without an explicit correction for gelbstoff, exhibits an opposite response in the $0.5\text{--}5 \text{ mg} \cdot \text{m}^{-3}$ chlorophyll *a* range, becoming more inaccurate as gelbstoff absorption increases (Fig. 2). The accuracy of the CZCS-style algorithm is highest at chlorophyll *a* concentrations of about $2.5 \text{ mg} \cdot \text{m}^{-3}$ (Fig. 2a), at intermediate levels of gelbstoff absorption, suggesting that similar water types were used in the derivation of this algorithm. Variations in the slope parameter *S* predictably result in different responses from the two algorithm types, although both indicate that variations in *S* must be considered in conjunction with the magnitude of absorption (Fig. 3). The semi-analytical algorithm responds most notably to divergence from the canonical slope parameter at the highest values of $a_g(400)$; it would appear that inaccuracies arising from slope divergence are only significant at high values of gelbstoff absorption. The CZCS-style algorithm similarly indicates that absorption magnitude, as a concentration proxy, is an important consideration in slope-related effects, although algorithm response is highly variable at different concentrations of chlorophyll *a*.

SUMMARY

The large variations in accuracy of the combined algorithm creates strong arguments for both regional validation programmes (Gordon and Morel 1983, Carder *et al.* 1991, Carder 1994) and an intelligent interpretation of ocean colour products as they become available. The tested semi-analytical algorithm appears to perform relatively well at low to moderate levels of biomass, i.e. $<3 \text{ mg} \cdot \text{m}^{-3}$ chlorophyll *a*, but its heightened tendency to failure above these concentrations indicates a lack of applicability to the Benguela upwelling system. Semi-analytical algorithms remain the optimal choice for derived ocean colour products, and new variants should be evaluated for regional application as they become available. However, given the unproved nature of semi-analytical algorithms at high biomass levels, it appears that a high priority must be given to both assessing and modifying empirical algorithms for

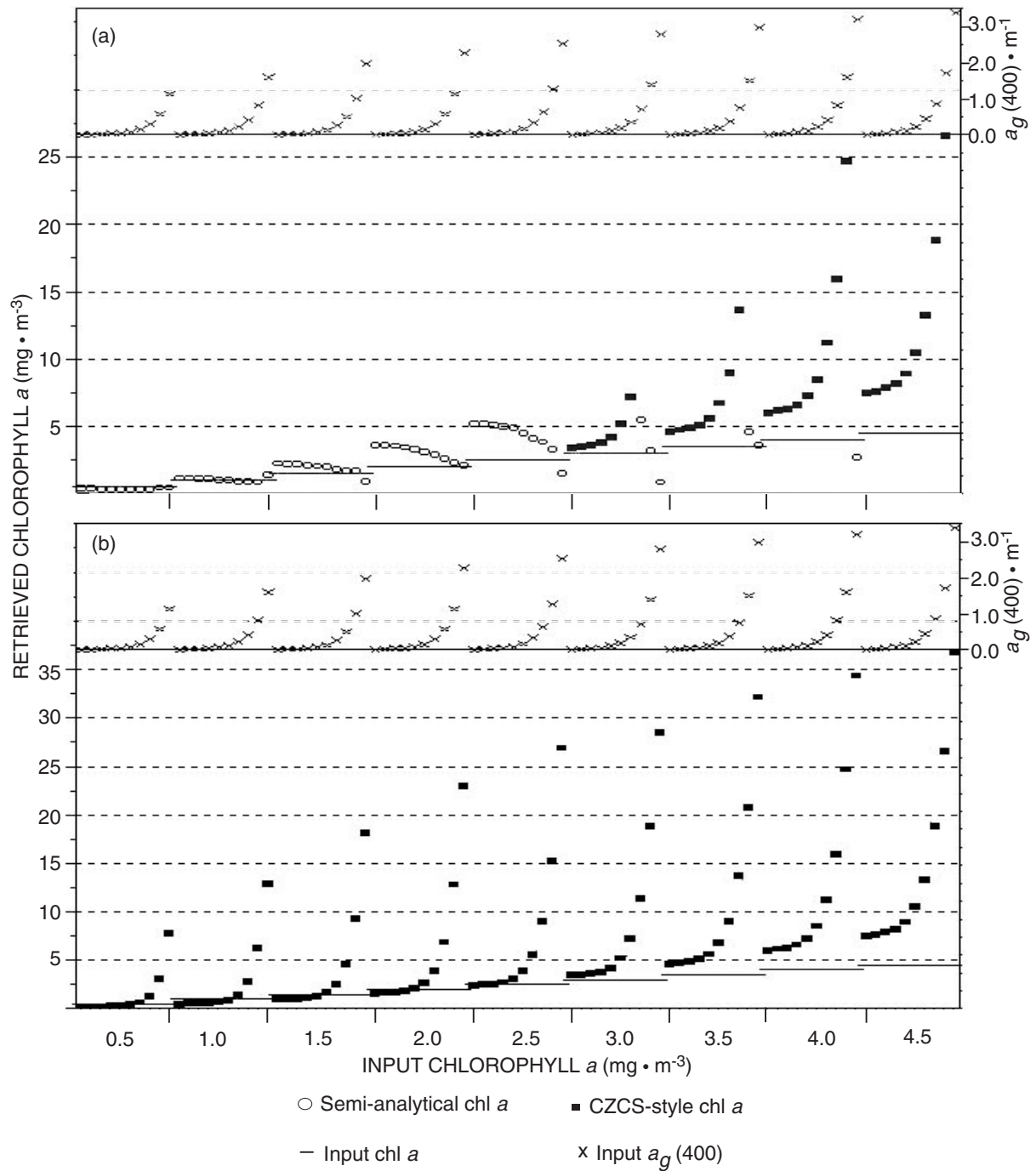


Fig. 2: Performance of SeaWiFS (a) combined algorithm and (b) empirically derived CZCS-style algorithm at 0.5–4.5 $\text{mg} \cdot \text{m}^{-3}$ chlorophyll a , at fixed S , and varying $a_g(400)$. Note the high failure rate of the semi-analytical algorithm above 3 $\text{mg} \cdot \text{m}^{-3}$ chlorophyll a

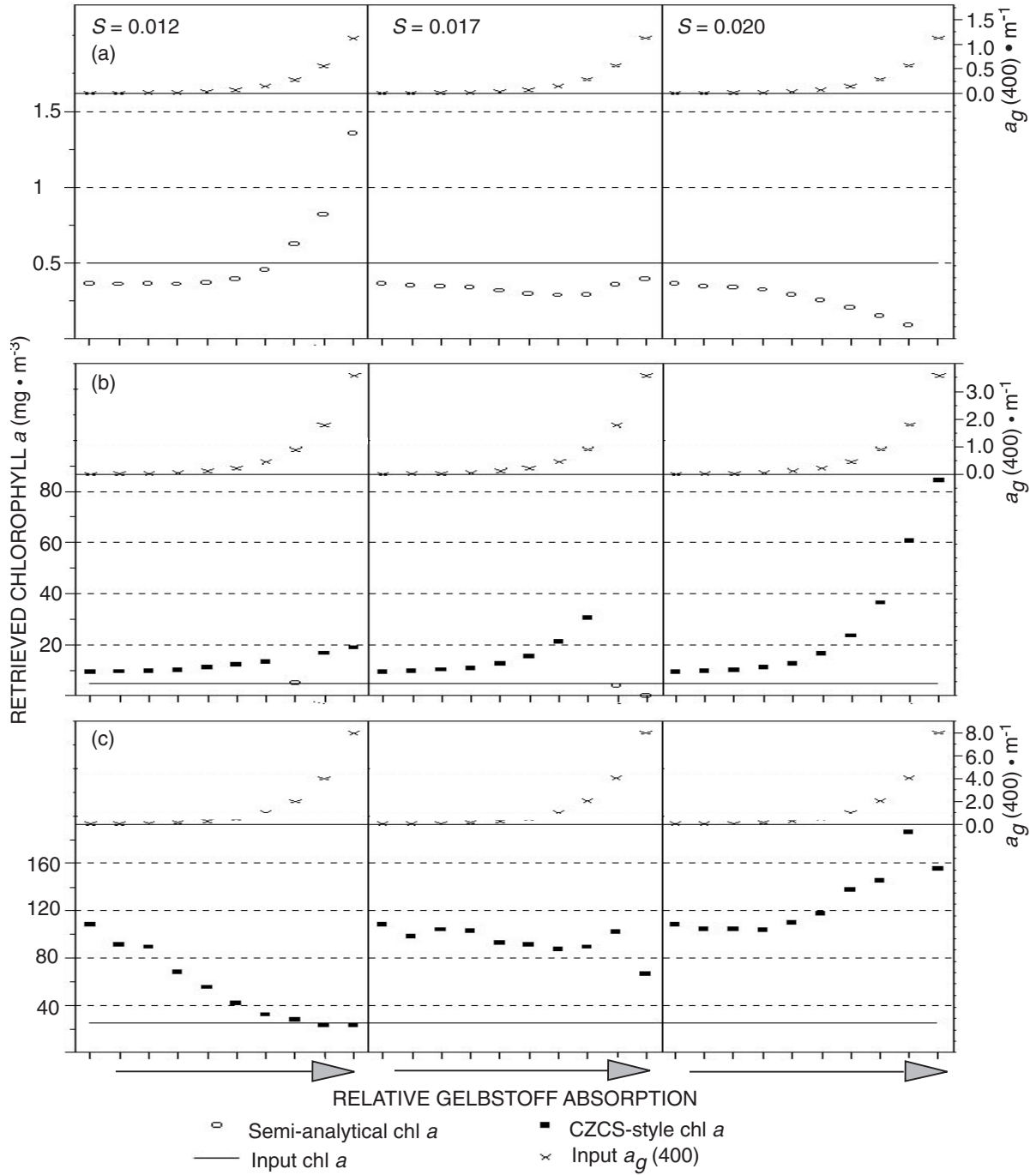


Fig. 3: Performance of SeaWiFS combined algorithm at (a) 0.5 mg·m⁻³ (b) 5 mg·m⁻³ and (c) 25 mg·m⁻³ chlorophyll *a*, at varying *S* and *a_g*(400)

default use regionally (e.g. Aiken *et al.* 1995). This is reinforced by the resource limitations facing southern African algorithm validation, as empirically derived CZCS-style algorithms may be validated more simply than their semi-analytical counterparts. Although devoted bio-optical validation programmes, measuring the response of the underwater light-field to variations in core bio-optical parameters, must continue if full potential of ocean colour data is to be realized (i.e. synoptic primary production data), resource limited validation, using available data in combination with bio-optical modelling, must also be initiated. This at least will allow the initial use of satellite-derived chlorophyll data in high biomass or bloom-type scenarios within known confidence limits.

Processing and interpretation of ocean colour data must be accompanied by detailed flagging routines, indicating which algorithm type has been used to calculate chlorophyll *a* concentrations. This is of particular importance in bloom-type scenarios, where switching of algorithm types can be expected in response to rapid variations in phytoplankton concentrations and associated degradation products. The data presented here indicate that high-level chlorophyll *a* products, e.g. Level 3 and above, that are not accompanied by adequate processing information, should be used with extreme caution in areas of mode-rate to high chlorophyll *a* biomass (>3 mg·m⁻³).

ACKNOWLEDGEMENTS

The senior author is grateful to Sea Fisheries for permission to participate on various research cruises and for other logistical support.

LITERATURE CITED

- AIKEN, J., MOORE, G. F., TREES, C. C., HOOKER, S. B. and D. K. CLARK 1995 — The SeaWiFS CZCS-type pigment algorithm. *SeaWiFS tech. Rep. Ser. NASA tech. Memo.* **29**: 34 pp.
- BIDIGARE, R. 1994 — Measurement of algal chlorophylls and carotenoids by HPLC. In *Protocols for the Joint Global Ocean Flux Study (JGOFS) Core Measurements. IOC/SCOR Manual and Guide* **29**: 91–96.
- BRICAUD, A., MOREL, A. and L. PRIEUR 1981 — Absorption by dissolved organic matter of the sea (yellow substance) in the UV and visible domains. *Limnol. Oceanogr.* **26**(1): 43–53.
- BRICAUD, A., BABIN, M., MOREL, A. and M. CLAUSTRÉ 1995 — Variability in the chlorophyll specific absorption coefficient of natural phytoplankton: analysis and parameterization. *J. geophys. Res.* **100**(C7): 13321–13332.
- BROWN, P. C. 1992 — Spatial and seasonal variation in chlorophyll distribution in the upper 30 m of the photic zone in the southern Benguela/Agulhas ecosystem. In *Benguela Trophic Functioning*. Payne, A. I. L., Brink, K. H., Mann, K. H. and R. Hilborn (Eds). *S. Afr. J. mar. Sci.* **12**: 515–525.
- CAMPBELL, J. W., BLAISDELL, J. M. and M. DARZI 1995 — Level-3 SeaWiFS data products: spatial and temporal binning algorithms. *SeaWiFS tech. Rep. Ser. NASA tech. Memo.* **32**: 73 pp.
- CARDER, K. L. 1994 — Case 2 Chlorophyll *a* Algorithm. MODIS Ocean Science Team. Algorithm Theoretical Basis Document ATBD-MOD-19. <http://eosps0.gsfc.nasa.gov/atbd/modis/atbdmod19new.html>.
- CARDER, K. L., STEWARD, R. G., HARVEY, G. R. and P. B. ORTNER 1989 — Marine humic and fulvic acids: their effects on remote sensing of ocean chlorophyll. *Limnol. Oceanogr.* **34**(1): 68–81.
- CARDER, K. L., HAWES, S. K., BAKER, K. A., SMITH, R. C., STEWARD, R. G. and B. G. MITCHELL 1991 — Reflectance model for quantifying chlorophyll *a* in the presence of productivity degradation products. *J. geophys. Res.* **96**(C11): 20599–20611.
- CARDER, K. L., LEE, Z., HAWES, S. K. and F. R. CHEN 1995 — Optical model of ocean remote sensing: application to ocean color algorithm development. In *COSPAR Colloquium. Space Remote Sensing of Subtropical Oceans (SRSSO)*. Taipei, Taiwan, September 1995: 15A3-1–15A3-6.
- COBLE, P. G. 1996 — Characterisation of marine and terrestrial DOM in seawater using excitation-emission matrix spectroscopy. *Mar. Chem.* **51**: 325–346.
- COBLE, P. G., GREEN, S. A., BLOUGH, N. V. and R. B. GAGOSIAN 1990 — Characterization of dissolved organic matter in the Black Sea by fluorescence spectroscopy. *Nature, Lond.* **348**: 432–435.
- COBLE, P. G., SCHULTZ, C. A. and K. MOPPER 1993 — Fluorescence contouring analysis of DOC intercalibration experiment samples: a comparison of techniques. *Mar. Chem.* **41**: 173–178.
- DE SOUZA SIERRA, M. M., DONARD, O. F. X., LAMOTTE, M., BELIN, C. and M. EWALD 1994 — Fluorescence spectroscopy of coastal and marine waters. *Mar. Chem.* **47**: 127–144.
- DETERMANN, S., REUTER, R., WAGNER, P. and R. WILLKOMM 1994 — Fluorescent matter in the eastern Atlantic Ocean. I. Method of measurement and near-surface distribution. *Deep-Sea Res.* **41**(4): 659–675.
- DONARD, O. F. X., BELIN, C. and M. EWALD 1987 — Corrected fluorescence excitation spectra of fulvic acids. Comparison with the UV/visible absorption spectra. *Sci. total Environment* **62**: 157–161.
- DRUFFEL, E. R. M., WILLIAMS, P. M., BAUER, J. E. and J. E. ERTEL 1992 — Cycling of dissolved and particulate organic matter in the open ocean. *J. geophys. Res.* **97**(C10): 15639–15659.
- EHRHARDT, M. 1984 — Marine gelbstoff. The handbook of environmental chemistry. In *The Natural Environment and the Biogeochemical Cycles* **1**(Part C). Hutzinger, O. (Ed.). Berlin; Springer: 63–77.
- FERRARI, G. M. and S. TASSAN 1991 — On the accuracy of determining light absorption by “yellow substance” through measurements of induced fluorescence. *Limnol. Oceanogr.* **36**(4): 777–786.
- GORDON, H. R. and A. Y. MOREL (Eds) 1983 — *Remote Assessment of Ocean Colour for Interpretation of Satellite Visible Imagery: a Review*. New York; Springer: 114 pp.
- GORDON, H. R., BROWN, O. B., EVANS, R. H., BROWN, J. W., SMITH, R. C., BAKER, K. S. and D. K. CLARK 1988 — A semianalytical model of ocean color. *J. geophys. Res.* **93**(D9): 10909–10924.
- GREEN, S. A. and N. V. BLOUGH 1994 — Optical absorption and fluorescence properties of chromophoric dissolved organic matter in natural waters. *Limnol. Oceanogr.* **39**(8):

- 1903–1916.
- HARVEY, G. R., BORAN, D. A., CHESAL, L. A. and J. M. TOKAR 1983 — The structure of marine fulvic and humic acids. *Mar. Chem.* **12**: 119–132.
- HAYASE, K. and H. TSUBOTA 1985 — Sedimentary humic acid and fulvic acid as fluorescent organic materials. *Geochim. cosmochim. Acta* **49**: 159–163.
- HOGUE, F. E., VODACEK, A. and N. V. BLOUGH 1993 — Inherent optical properties of the ocean: retrieval of the absorption coefficient of chromophoric dissolved organic matter from fluorescence measurements. *Limnol. Oceanogr.* **38**(7): 1394–1402.
- LEE, Z., CARDER, K. L., HAWES, S. K., STEWARD, R. G., PEACOCK, T. G. and C. O. DAVIS 1994 — Model for the interpretation of hyperspectral remote-sensing reflectance. *Appl. Opt.* **33**(24) : 5721–5732.
- MOPPER, K. and C. A. SCHULTZ 1993 — Fluorescence as a possible tool for studying the nature and water column distribution of DOC components. *Mar. Chem.* **41**: 229–238.
- MOREL, A. 1988 — Optical modeling of the upper ocean in relation to biogenous matter content (Case I waters). *J. geophys. Res.* **93**(C9): 10749–10768.
- MUELLER, J. L. and R. W. AUSTIN 1995 — Ocean optics protocols for SeaWiFS validation, revision 1. *SeaWiFS tech. Rep. Ser. NASA tech. Memo.* **25**: 40–42.
- NELSON, J. R. and S. GUARDA 1995 — Particulate and dissolved spectral absorption on the continental shelf of the southeastern United States. *J. geophys. Res.* **100**(C5): 8715–8732.
- PEACOCK, T. P., CARDER, K. L. and R. G. STEWARD 1988 — Components of spectral attenuation for an offshore jet in the California coastal transition zone. *Eos* **69**(44): p. 1125.
- SIEGEL, D. A. and A. F. MICHAELS 1996 — Quantification of non-algal light attenuation in the Sargasso Sea: implications for biogeochemistry and remote sensing. *Deep-Sea Res. II* **43**(2–3): 321–345.
- SMITH, R. C. and K. S. BAKER 1981 — Optical properties of the clearest natural waters (200–800 nm). *Appl. Opt.* **20**: 177–184.